

BABEȘ BOLYAI UNIVERSITY
FACULTY OF PHYSICS



PH.D. THESIS SUMMARY

**Order-disorder transitions in
coupled oscillator systems**

Author:
BODA Szilárd

Supervisor:
Prof. Dr. NÉDA Zoltán

CLUJ-NAPOCA 2013

Contents

1	Emerging synchronization - general aspects	4
2	Classical models of spontaneous synchronization	4
2.1	Introduction	4
2.2	Kuramoto model	5
2.3	Integrate and fire type oscillators	5
2.4	Two-mode stochastic oscillators	6
3	Synchronization of two mode stochastic oscillators	7
3.1	Novel simulations for variable waiting periods (model I)	7
3.2	Results for the modified model (model II) with variable emitting periods	8
3.3	Experimental realization of the two-mode stochastic oscillator system	9
3.4	Experimental results for the first model	10
3.5	Experimental results for the second model	10
4	Synchronization studies in globally coupled metronome systems	10
4.1	Introduction	10
4.2	Experimental setup	11
4.3	Synchronization of coupled metronome systems	12
4.3.1	Experimental Results	12
4.3.2	A theoretical model	13
4.3.3	Realistic metronome parameters	14
4.3.4	Validation of the model	14
4.3.5	Synchronization of two metronomes	15
4.4	Further theoretical analysis	15
4.5	Exemplifying the Kuramoto-type phase transition with metronomes	16
4.5.1	Experimental setup and results	16
4.5.2	Theoretical model	17
4.5.3	Numerical results	18
5	Summary	19
6	Relevant personal contributions	21
	Selected References	22

Thesis outline

The present thesis is structured in four main parts.

In the first part, consisting of Chapter I and II we give a literature review about the synchronization phenomena. In Chapter I (entitled **Emerging synchronization - general aspects**) we present a historical review about the problematics of spontaneous synchronization. In Chapter II (entitled **Classical models of spontaneous synchronization**) we describe the main models which aim to explain spontaneous synchronization. We argue on the importance of these models, we present the Kuramoto, the integrate and fire and the two-mode stochastic oscillator models.

In the second part, consisting of Chapter III (entitled **Synchronization of two mode stochastic oscillators**) we present our research, related to the two-mode stochastic oscillators. We present a new optimized algorithm for simulating such systems, we introduce a novel type of two-mode stochastic oscillators and investigate it's behavior for different parameters. We describe an experimental realization of the system and present results obtained with it. Experimental and theoretical results are compared in a critical manner.

The third part contains Chapter IV and V. In Chapter IV (**Synchronization studies in globally coupled metronome systems**) we investigate the emergence of synchronization in a system composed of coupled metronomes. We give a historical introduction to these kind of setups. and describe the system we investigate experimentally. The system is modeled theoretically. By choosing realistic model parameters we reproduce the experimental results. Finite size effects are investigated by the theoretical model. In Chapter V (**Exemplifying the Kuramoto-type phase transition with metronomes**) we reproduce the Kuramoto-type phase transition with metronomes. We describe the used experimental method, the obtained experimental results and the theoretical model of the system. Experimental and theoretical results are compared and discussed.

In the fourth part, consisting of Chapter VI (**Summary**), Chapter VII (**Relevant personal contributions**) we summarize our results, discuss their relevance and enumerate the personal contributions. The thesis end with a Bibliography consisting of 44 titles.

Acknowledgements

I would first thank to the Lord, Who gave me the wisdom and the strength to successfully complete this research.

I am very grateful to my supervisor, Prof. Dr. Néda Zoltán, for offering me new perspectives in the field of physics. Without his excellent supervising, brilliant ideas and endless patience I wouldn't manage to overcome all the difficulties.

I want to thank to my colleagues from the Babes-Bolyai University, who helped me in my research: Dr. Arthúr Tunyagi, who designed and built the experimental setups, Botond Tyukodi, who helped me in the experimental part and also had brilliant ideas, Lect. Dr. Lázár Zsolt, who gave valuable programming advices. I also thank to my advising committee, Prof. Dr. Nagy László and Járαι-Szabó Ferenc for their help and support.

This work was possible with the financial support of the Sectoral Operational Programme for Human Resources Development 2007-2013, co-financed by the European Social Fund, under the project number POSDRU/107/1.5/S/76841 with the title Modern Doctoral Studies: Internationalization and Interdisciplinarity.

Last, but not least I want to thank to my girlfriend, my family and my friends for their support and encouragement.

Keywords

synchronization, collective behavior, phase-transition, coupled oscillators, coupled metronomes, stochastic oscillators, multi-mode oscillators

1 Emerging synchronization - general aspects

Spontaneous synchronization is a complex phenomena emerging in mechanical systems (pendulum clocks [3, 1, 4], mechanically coupled metronomes [10, 15]), biology (pacemaker cells [11], fireflies in south-east Asia [12]), and social systems (menstrual cycles of women living together [6], human clapping [9]). Because of the complexity and the variety of the systems in which synchronization emerges, it attracted the interest of scientists for centuries and even nowadays it is still an active research topic [14, 13].

The earliest scientifically documented work related to synchronization dates back to a dutch physicist in XVII century, Christiaan Huygens. He observed the synchronized motion of two of his pendulum clocks attached to the same wall, and mentioned this ”*sympathy of two clocks*” to his father, in a letter dated on 26 February 1665 [3].

He performed several experiments to find the origin of coupling between the pendulum clocks, and came to the conclusion, that the coupling is realized through tiny vibrations in their common suspension. He summarized his observations in a letter to the Royal Society of London [2].

Despite the fact, that Huygens made this discovery in the mid 17th century, mathematical models aimed to describe this appeared just after 1960, and surprisingly were elaborated by biologists.

Arthur Taylor Winfree in 1966 came to the conclusion that spontaneous synchronization is governed by the coupling strength between the oscillators, and appears as a genuine phase transition above a critical coupling value [16]. Kuramoto and Nishikawa[5] reformulated and simplified his model in order to make it analytically solvable.

Charles S. Peskin modeled the synchronization of pacemaker cells with a simple physical setup consisting of parallelly coupled capacitors and resistors [11]. Inspired by this model Mirollo and Strogatz made a more general model, which was simple enough to allow for analytical results [7].

2 Classical models of spontaneous synchronization

2.1 Introduction

Modeling and explaining such a fascinating and puzzling phenomena as emerging synchronization was not an easy task. We will present the basic biologically inspired models and we will introduce our novel modeling paradigm, which could be relevant for understanding spontaneous synchronization in biological or social systems.

2.2 Kuramoto model

Starting from Winfree’s model, which could not be solved analytically, in the 1980s Yoshiki Kuramoto and Ikuko Nishikawa [5] developed the Kuramoto model, which is a mathematical model for describing the collective behavior of an ensemble of phase coupled non-identical rotators. In the best known formulation every rotator has its own, intrinsic ω_i frequency, which is distributed according to a $g(\omega_i)$ probability density. The coupling between the oscillators is uniform and global. The evolution of the system is given by:

$$\frac{\partial \theta_i}{\partial t} = \omega_i + \frac{K}{N} \sum_{j=1}^N \sin(\theta_j - \theta_i), i = 1 \dots N. \quad (1)$$

where N is the number of the oscillators, K is the coupling constant, and θ_i is the phase of unit i . In order to characterize the level of the synchronization in the system it is crucial to work with a proper order parameter. Kuramoto *et. al.* came to the conclusion that a suitable order parameter, r , for their system would be:

$$r \exp(i\psi) = \frac{1}{N} \sum_{j=1}^N \exp(i\theta_j), \quad (2)$$

where ψ represents a kind of collective phase of the synchronized state.

The Equations can be solved exactly, and one can find a K_c critical value, above which synchronization appears.

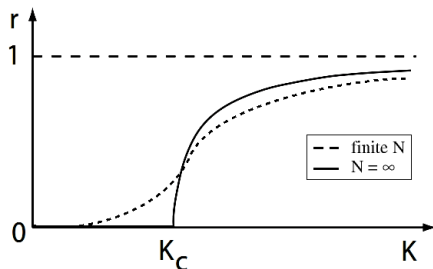


Figure 1: Results for the order-parameter of the Kuramoto model.

If $K < K_c$ the system will be in a disordered phase, where the units are not synchronized, and $r = 0$. The transition from the unsynchronized state to the synchronized one appears as a second order phase-transition (as it is sketched in Figure 1.)

2.3 Integrate and fire type oscillators

The disadvantage of the Kuramoto model is that the interactions between the oscillators are continuously acting. In biological systems, however, it is more

relevant to have pulse-like interactions, i.e. the interaction is present only for a limited part of the period. Starting from Charles S. Peskin model[11] in 1990 Mirolo and Strogatz developed a more general theoretical model [7].

They considered a globally coupled oscillator ensemble with pulse-like interactions. They associated a Φ phase parameter to each oscillator. When the oscillator reaches the maximum Φ value, it will emit a pulse (will fire) and the value of the parameter will become 0, after which the cycle starts again. They also associated an energy type parameter, E , to the oscillator which is linked to the phase parameter through a monotonic function: $E = f(\Phi)$. If one oscillator fires, the effect of the emitted pulse on the other oscillators will be, that their energy parameter will be instantaneously increased by a σ value. By increasing the value of E , the value of Φ will increase consecutively, shortening the time until the oscillator fires. If we illustrate the oscillators as points moving along the f function then we can observe their dynamics on Figure 2.

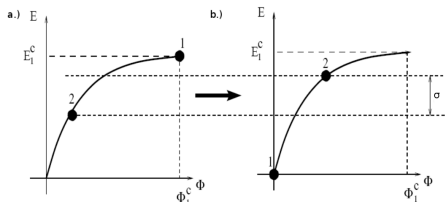


Figure 2: *The dynamics of two integrate and fire type oscillator. a.) Oscillator 1 is at the maximum phase value, oscillator 2 is below b.) oscillator 1 fires, and raises the energy of oscillator 2 with a σ value.*

If we imagine the oscillators as an interacting ensemble and not just individual specimens, then we will immediately come to the conclusion, that the firing of one oscillator can trigger an avalanche of firings, until all the oscillators will fire in unison (similar to the fireflies, or the pacemaker cells). Depending on the difference between the oscillators, there is a critical σ_c coupling constant. If $\sigma > \sigma_c$ the oscillators will synchronize.

Both the Kuramoto model and the integrate and fire oscillator models have a built-in phase minimizing mechanism, so the appearance of spontaneous synchronization is an expected phenomenon.

2.4 Two-mode stochastic oscillators

In complex biological and sociological systems we do not know whether synchronization is the primary aim of the participating specimens, or appears only as a co-product of a hidden optimization mechanism. With the hope of better understanding this issue, Nikitin, Vicsek and Néda [8] introduced and investigated a new type of oscillator ensemble, the pulse coupled two mode stochastic oscillator system.

They have considered a quite general oscillator family, where the oscillator

periodically cycles between three possible phases, A , B , and C . The first phase (A) is a stochastic state. The remaining two states (B and C) are deterministic. The B state is a waiting period, which in the case of neurons corresponds to a relaxation and recombination process. State C is the pulse emitting phase, here the oscillators fire, or emit a pulse. They denoted with τ_A , τ_B and τ_C the time periods which the oscillator spent in the respective states.

The emitting state is state C . Here the oscillator will emit a constant pulse of intensity $\frac{1}{N}$, where N is the number of oscillators. The total output of the system is:

$$f = \sum_{i=1}^N f_i, \quad (3)$$

where f_i is the output of oscillator i , which has the following values:

$$f_i = \begin{cases} 0 & \text{if the oscillator is in state A or B} \\ \frac{1}{N} & \text{if the oscillator is in state C} \end{cases}$$

Every oscillator detects the pulses emitted by the others, so they are globally coupled. The governing dynamics is simple: the oscillators try to maintain the total output of the system, f , around a given f^* value. In order to achieve this, the oscillators can play with two different modes by manipulating the emitted pulses. This pulse manipulation can be done in two different ways: either with variable waiting periods, or variable emitting periods. In both scenarios, for certain parameter intervals a partial synchronization will emerge.

3 Synchronization of two mode stochastic oscillators

3.1 Novel simulations for variable waiting periods (model I)

As a first exercise we have tried to reproduce with optimized computer simulation the results published in the work of Nikitin, Vicsek and Nédá in 2003. Fixing the appropriate parameters ($\tau_{B_1} = 0.8$ s, $\tau_{B_{11}} = 0.4$ s, $\tau_c = 0.1$ s and $\tau_* = 0.2$ s) we ran simulations for different oscillator numbers and f^* values. We calculated the equilibrium synchronization level and averaged the results for 100 runs, each with different initial conditions. The overall results for the synchronization order parameter as a function of f^* is plotted in Figure 3.

Our results suggests that as a function of f^* the system will go from an unsynchronized state to a synchronized one, and then back again to an unsynchronized state. The sudden change in the order parameter indicates two phase-transition like phenomena, which becomes more evident, as the number of oscillators are increased. The obtained results are in very good agreement with the ones obtained in the previous studies by Nikitin, Vicsek and Nédá, giving thus confidence in the optimized numerical code in further studies.

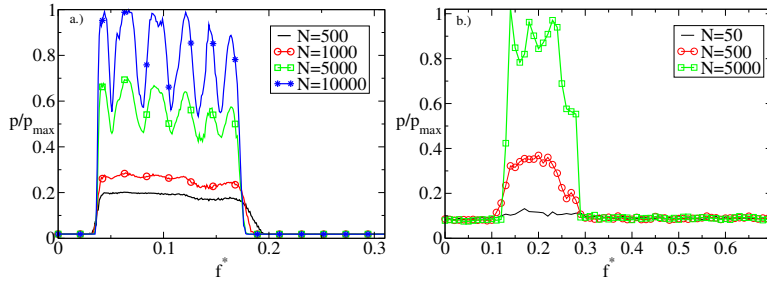


Figure 3: *Simulation results for the two mode stochastic oscillators with a) two possible waiting periods. b) variable emitting periods*

3.2 Results for the modified model (model II) with variable emitting periods

To prove that synchronization through optimization is a more general concept, and it does not appear only in the very strict model used previously, we considered another variant of the model. The dynamics of these new oscillators is similar to the previous case, but instead of variable waiting periods, we have two possible emitting periods. We have chosen parameter values close to our previous model, and fixed: $\tau_B = 0.4$ s, $\tau_{C_I} = 0.1$ s, $\tau_{C_{II}} = 0.2$ s and $\tau^* = 0.2$ s. We ran multiple simulations, and calculated the order parameter, averaging the results over several runs. The averaged results can be seen on Figure 3.

We investigated the dependence of the oscillator numbers on the detected synchronization level, considering up to $N = 5000$ oscillators. The obtained results are presented on Figure 4. Although there is a fluctuation in the order parameter, we have a very clear trend: by increasing the number of oscillators, the synchronization level rises.

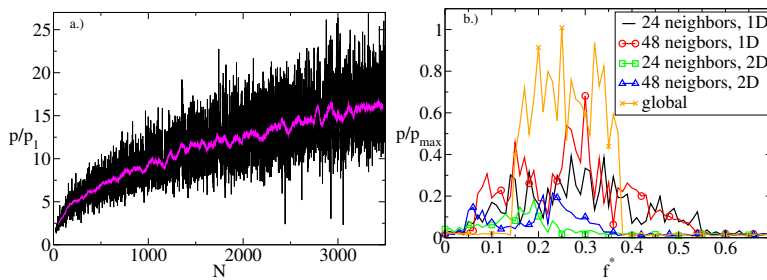


Figure 4: *Simulation results for the two mode stochastic oscillators with variable emitting periods. a) for different numbers of oscillators, the black line is the raw result, the red one is an averaging on a moving window with length $\Delta N = 50$. $f^* = 0.15$ s and $\tau^* = 0.2$ s b) Results for 1D and 2D square lattice and local coupling ($N=2500$, $\tau_A = 0.08$ s, $\tau_B = 0.8$ s, $\tau_{C_I} = 0.2$ s, $\tau_{C_{II}} = 0.4$ s).*

We also studied how the topology of the coupling influences the synchronization level. Instead of the global coupling, we considered a local coupling with a lattice topology. Synchronization may emerge under certain f^* intervals, for high number of interacting neighbors. For low number of interacting neighbors synchronization will not appear. On Figure 4 we present results in such a case, using $N = 2500$ oscillators.

3.3 Experimental realization of the two-mode stochastic oscillator system

Here we consider an experimental realization of the two-mode stochastic oscillator system. To accomplish our goal we designed a new type of oscillator, and we named them as “electronic fireflies”. The oscillators and the computer interface for measurements was designed, built and programmed by Dr. Arthúr Tunyagi. These electronic fireflies have three main properties:

1. they can emit a light pulse with a Light Emitting Diode (LED)
2. they can detect the light intensity through a photo-resistor.
3. the dynamical behavior of the firefly is governed by an Atmega8 micro-controller

On Figure 5 we present the circuit board with the electronic fireflies on it and the computer interface powered by a power supply.

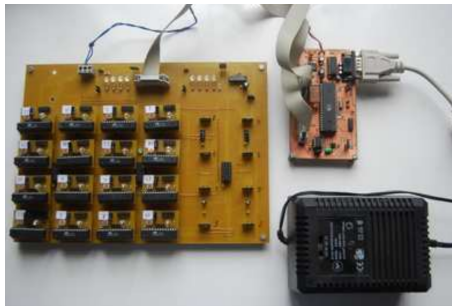


Figure 5: *The circuit board with the electronic fireflies and the computer interface.*

We investigated both types of oscillators with this experimental setup: oscillators with variable waiting periods and oscillators with variable emitting periods. By shifting between these variable periods (between the waiting periods in the first model, and between the emitting periods in the second model) the oscillators try to maintain the total output of the system around a given threshold value. As a co-product of this simple optimization rule a nontrivial synchronization emerged for certain parameter intervals.

3.4 Experimental results for the first model

The order parameter was calculated in the same manner as in simulations. The obtained order parameter as a function of the reference voltage, U (having the role of the f^* parameter), for different numbers of fireflies is plotted in Figure 6.

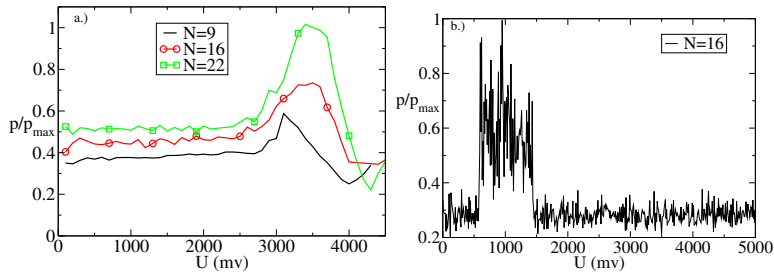


Figure 6: *Processed experimental results for the detected synchronization level a) for the first model b) for the second model*

Similarly with the results obtained in the simulations, we can observe an emerging synchronization, and by increasing the number of electronic fireflies, the level of synchronization rises. The appearance and disappearance of the synchronization suggests a phase transition, which is more evident as the size of the system is increased.

3.5 Experimental results for the second model

In this case we slightly modified the program governing the dynamics of the fireflies, and burned the program into the fireflies EEPROM. Similarly to the previous case, we processed the obtained data, and calculated the order parameter. The obtained order parameter as a function of the U threshold value for the used 16 fireflies can be seen on Figure 6.

The trend in the order parameter suggests that the system undergoes two transitions: one from an unsynchronized state to a synchronized one, and another one from a synchronized to an unsynchronized one, as we increase the reference voltage. The sharp change observable in the variation of the order parameter as a function of U suggests a phase transition.

4 Synchronization studies in globally coupled metronome systems

4.1 Introduction

Since Huygens many scientists revisited Huygens original experiment ([1], [4] etc.)

The most complete analysis for Huygens' clocks was made by Kapitaniak *et. al.* [4]. They also confirmed, that the anti-phase synchronization is the dominant collective behavior [4].

Inspired by Huygens's pendulum clock system, Pantaleone [10] proposed a simple mechanical setup for exemplifying the Kuramoto model. Instead of pendulum clocks, his setup was composed by two metronomes placed on a light, easily movable platform.

Pantaleone monitored the metronomes by recording their sound. Pantaleone found just in-phase synchronization for the metronomes and derived also approximate equations of motion for the time-evolution of the metronome ensemble.

Ulrichs *et. al.* [15] reconsidered theoretically Pantaleone's experiment and considered larger metronome numbers. They also confirmed the absence of anti-phase synchronization for metronomes.

We considered a similar setup, but instead of a light wooden platform placed on two cylinders we used a rotating disk shaped platform.

4.2 Experimental setup

Our setup consist of metronomes uniformly distributed on the perimeter of a rotating disk. es.

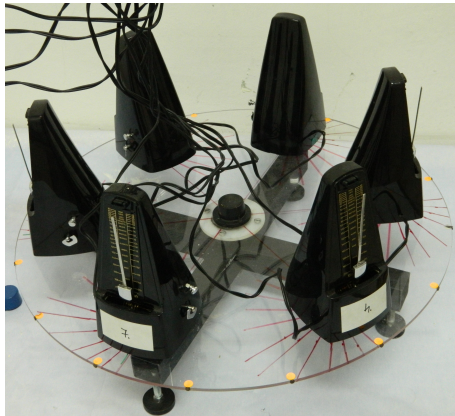


Figure 7: *The experimental setup.*

To monitor the movement of the metronomes' bobs we considered a simple and cheap solution, by mounting Kingbright KTIR 0611 S photo-cell detectors in their trajectory.

In order to numerically characterize the synchronization level we used the Kuramoto order parameter [5]:

$$r \exp(i\phi) = \frac{1}{N} \sum_j \exp(i\theta_j). \quad (4)$$

4.3 Synchronization of coupled metronome systems

In this section we will experimentally and theoretically investigate the conditions favoring synchronization in our setup.

4.3.1 Experimental Results

Starting from 160 BPM's, we have scanned all the nominal frequency values up to 208 BPM (168, 176, 184, 192 and 208 BPM's). We considered 10 independent measurement for each frequency, calculated the Kuramoto order parameter, and averaged the values obtained for the same frequency. The obtained results are presented in Figure 8a.

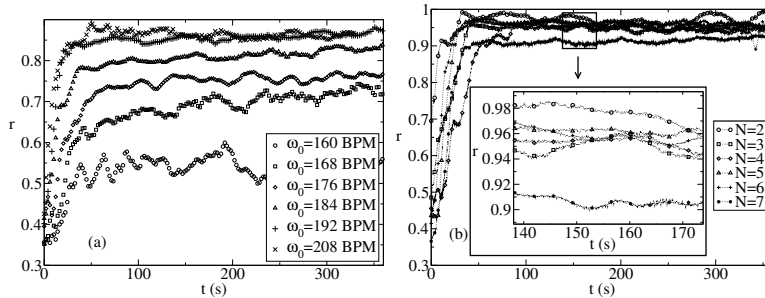


Figure 8: Evolution of the averaged Kuramoto order parameter for a) different natural frequencies and $N = 7$ metronomes. b) different metronome number and for $\omega_0 = 192$ BPM.

The results suggest that the obtained degree of synchronization increases as the metronomes' natural frequency increases. To investigate whether this is due to a change in the standard deviation of the metronomes' frequencies, we also measured the standard deviation between the metronomes' natural frequencies but we came up with roughly constant values. So we can affirm, that the monotonically increasing trend of the synchronization level, as a function of the nominal frequency of the metronomes, is not due to the changes in the metronomes' natural frequencies standard deviation.

Secondly we investigated how the metronomes number influences the synchronization level in the system. We proceed in a similar manner as in the previous case, with the sole difference that now we fixed the frequency ($\omega_0 = 192$ BPM) and after performing the 10 measurements we consecutively removed one metronome from the platform. The averaged results are plotted in Figure 8. We can see, that by increasing the number of metronomes, the level of the synchronization will monotonically decrease.

We calculated again the standard deviation of the metronomes' natural frequencies in this case and there was not a clear trend as a function of the number of metronomes, N , so we can affirm that the decreasing trend of the synchronization level as a function of the metronomes' number is not due to the variation

in the dispersion of the metronomes' frequencies.

4.3.2 A theoretical model

In order to study such systems in a more flexible manner, we developed a realistic theoretical model. We considered a simple mechanical model, which takes into consideration only the essential parts of the system. The starting elements are: a rotating platform and physical pendulums attached to its perimeter.

For such a simple mechanical setup it is easy to write the Lagrange function, which will be:

$$L = \frac{J}{2}\dot{\phi}^2 + \sum_{i=1}^N \frac{J_i\omega_i^2}{2} + \sum_{i=1}^N \frac{m_i}{2} \left\{ \left[\frac{d}{dt} (x_i + h_i \sin \theta_i) \right]^2 + \left[\frac{d}{dt} (h_i \cos \theta_i) \right]^2 \right\} - \sum_{i=1}^N m_i g h_i (1 - \cos \theta_i) \quad (5)$$

In the Lagrangian we have used the following notations: the index i denotes the pendulums, J is the moment of inertia of the platform with the metronomes on it - taken relative to the vertical rotation axes, ϕ is the angular displacement of the platform, J_i is the moment of inertia of the pendulum relative to its center of mass, ω_i is the angular velocity of the rotation of the pendulum relative to its center of mass, m_i is the total mass of the pendulum ($m_i \approx W_1^{(i)} + W_2^{(i)}$, neglecting the mass of the rod), x_i is the horizontal displacement of the center of mass of the pendulums due to the rotation of the platform, h_i is the distance between the center of mass and the suspension point of the pendulum and θ_i is the displacement of the i -th pendulum's center of mass, in radians. For further simplifications we assumed, that the weights suspended on the metronomes' bobs are identical ($W_1^{(i)} = w_1$, $W_2^{(i)} = w_2$, and $m_i = m$), and we disregarded the $m_i g h_i$ constant term which will disappear after the derivation. Taking in consideration, that $x_i = R\dot{\phi}$ and $\omega_i = \dot{\theta}_i$, the Euler-Lagrange equations will be:

$$(J + NmR^2)\ddot{\phi} + mR \sum_i h_i [\ddot{\theta}_i \cos \theta_i - \dot{\theta}_i^2 \sin \theta_i] = 0 \quad (6)$$

$$[mh_i^2 + J_i]\ddot{\theta}_i + mR\dot{\phi}h_i \cos \theta_i + mgh_i \sin \theta_i = 0.$$

Adding now friction and driving terms, the Euler-Lagrange equations will yield:

$$(J + NmR^2)\ddot{\phi} + mR \sum_i h_i [\ddot{\theta}_i \cos \theta_i - \dot{\theta}_i^2 \sin \theta_i] + c_\phi \dot{\phi} + \sum_i \mathbb{M}_i = 0 \quad (7)$$

$$[mh_i^2 + J_i]\ddot{\theta}_i + mR\dot{\phi}h_i \cos \theta_i + mgh_i \sin \theta_i + c_\theta \dot{\theta}_i = \mathbb{M}_i. \quad (8)$$

Here c_ϕ is the friction coefficient for the rotation of the platform and c_θ the friction coefficient characterizing the pendulums movement. The \mathbb{M}_i term is the driving, for which we used the following form:

$$\mathbb{M}_i = M\delta(\theta_i)\dot{\theta}_i, \quad (9)$$

where δ denotes the Dirac function and M is a fixed parameter characterizing the driving mechanism of the metronomes.

In order to model the deviations in the metronomes' natural frequency we added a Gaussian noise in the L_2 terms, and considered the L_1 distances fixed and identical for all the metronomes.

4.3.3 Realistic metronome parameters

A challenge in this research was to find the realistic model parameters for the metronomes. First we determined the measurable ones with a help of an analytical balance ($w_1 = 0.025 \text{ kg}$, $w_2 = 0.0069 \text{ kg}$), and a caliper ($L_1 = 0.0358 \text{ m}$, $L_2 \in [0.019, 0.049] \text{ m}$ depending on the chosen natural frequency, $R = 0.27 \text{ m}$) and calculated $J \in [0.0729, 0.25515] \text{ kg m}^2$ depending on the number of metronomes placed on the platform. By adjusting in our simulations the value of the excitation and the friction coefficients until the same amplitudes are obtained for the pendulums and for the platform as in the experiments we found the realistic parameters. ($c_\theta = 5 \cdot 10^{-5} \text{ kg m}^2/\text{s}$, $c_\phi = 1 \cdot 10^{-5} \text{ kg m}^2/\text{s}$ and $M = 6 \cdot 10^{-4} \text{ Nm/s}$.)

4.3.4 Validation of the model

We numerically integrated the equations of motion (7),(8) with a velocity Verlet-type algorithm. For getting accurate results we considered a time-step of $dt = 0.01 \text{ s}$, and the simulations were performed up to a $t = 4000 \text{ s}$. We considered the same setup as in the experiments, and for the sake of better accuracy we considered 100 simulations with different initial conditions for each case, and averaged the results. The averaged results are presented in Figure 9a.

We can observe, that the obtained simulation trends are in good agreement with the experimental results presented earlier (Figure 8).

As a second validation step we studied the time-evolution of the order parameter for different numbers of pendulums, setting the same $\omega_0 = 192 \text{ BPM}$ natural frequency as in the experiments. We averaged the results for 100 independent simulations. The obtained curves are plotted in Figure 9. The simulated trend is again similar to the experimental one: increasing the number of metronomes results in a decrease in the observed synchronization level.

The simulation results suggest that our model with realistic model parameters describes well the dynamics of the coupled metronome system. Now we can investigate several interesting cases that are not feasible experimentally.

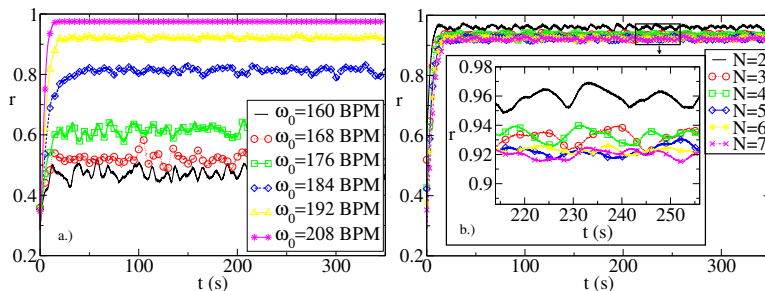


Figure 9: *Simulation results for the dynamics of the averaged Kuramoto order-parameter for: a) the same ω as the ones used in the experiments, for $N = 7$ metronomes. b) a fixed $\omega_0 = 192$ BPM and same number of pendulums that were used in the experiments.*

4.3.5 Synchronization of two metronomes

In all our experiments only in-phase synchronization appeared, and we felt the necessity to argue why this synchronization form is dominant in these kind of setups. We considered three different cases, 1. without driving and damping, 2. with a small driving and damping and 3. with realistic friction and excitation values. As one would naturally expect, for the friction-free and undriven case synchronization occurs only if the metronomes start either in completely in-phase or completely anti-phase configurations. If we add dissipation and driving, than for small dissipation and driving values the in-phase and anti-phase regions will be equally probable, but for realistic parameters the anti-phase synchronization will disappear, and will occur only in the case when the two metronomes are started exactly in anti-phases, yielding an unstable fix-point of the system.

4.4 Further theoretical analysis

Using our model we can consider a higher number of metronomes or investigate the system for more values of the metronomes' natural frequencies. The averaged results for a wide range of the number of metronomes, N , are presented in Figure 10 a.

It is easy to observe from Figure 10 that, in the $N \rightarrow \infty$ limit, a clear phase-transition like phenomenon emerges. In the neighborhood of the critical value of $\omega_c = 185$ BPM the order parameter exhibits a sharp increase, which becomes sharper and sharper as the number of metronomes are increased. This is a clear sign of phase-transition like behavior. To prove this, we also plotted the standard deviation of the order parameter values obtained from different simulations (Figure 10 b). We can see the characteristic peak around the $\omega_c = 185$ BPM value.

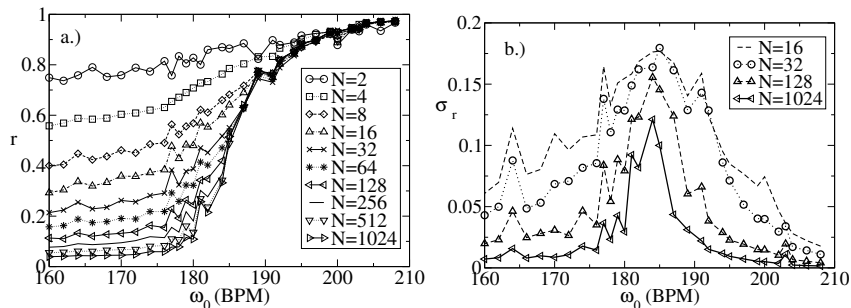


Figure 10: *Simulation results for the Kuramoto order parameter (a) and its standard deviation, σ_r , for the 100 computational experiments (b) as a function of the ω_0 frequency.*

4.5 Exemplifying the Kuramoto-type phase transition with metronomes

In the previous chapter we investigated experimental conditions favoring synchronization of the metronomes. In this section we want to investigate the influence of coupling between the metronomes, and we will try to reproduce in a pedagogical manner the Kuramoto-type phase transition using this system.

4.5.1 Experimental setup and results

We considered the very same setup as in the previous set of experiments, with three small changes:

1. a needle is mounted on the bottom of the metronomes, perpendicular to the pendulums swinging plane
2. on the platform where the metronomes are placed different orientation angles are marked with a step of 15 degrees from 0 to 180
3. metronomes are rotated by α angle in respect to the radial direction of the disk.

The main source of coupling in our system are the pulses given by the driving mechanism of the metronomes. The pulses can be easily decomposed in two components, a parallel one to the radial direction on the disk (p_{\parallel}) and a perpendicular one to this direction (p_{\perp}). By rotating the metronomes in respect to the radial direction of the disk, we will be able to decrease the p_{\perp} terms which in turn will decrease the coupling.

We carried out experiments for 2, 3 and 6 metronomes for different rotation angles starting from $\alpha = 0$ to $\alpha = 180$ with a step of 15 degrees (360 experiments overall). We computed the Kuramoto order parameter and averaged the results. The averaged results are illustrated on Figure 11.

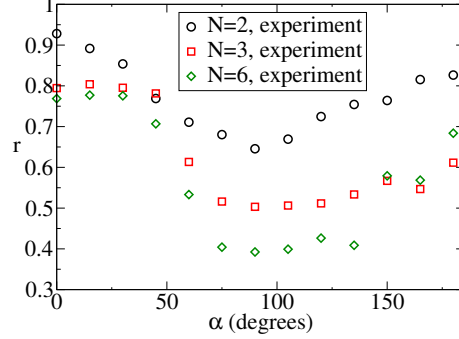


Figure 11: *Experimental results for the equilibrium synchronization level of the system for different orientation of the metronomes on the rotating platform.*

The curves suggests an order-disorder type phase-transition around $\alpha \approx 50^0$ and another transition around $\alpha \approx 150^0$. The first transition from the partially synchronized state to an unsynchronized one appears as a result of the decreased coupling strength. The asymmetric nature of the curve is due to the fact, that for $\alpha > 90^0$ the metronomes bob gets closer to the rotation axis of the disk, leading to a decrease in the torque produced by the p_{\perp} pulse. In agreement with the expected finite-size effects, by increasing the metronomes number on the disk, sharper and sharper transition curves are observable.

4.5.2 Theoretical model

By modifying the model to incorporate the rotation of the metronomes the Lagrangian of the system without driving and damping will write as

$$\begin{aligned}
L = & \frac{J}{2}\dot{\phi}^2 + \sum_{i=1}^N \frac{m_i}{2} \left\{ \left[\frac{d}{dt}(x_i \cos \alpha_i + h_i \sin \theta_i) \right]^2 + \left[\frac{d}{dt}(x_i \sin \alpha_i) \right]^2 + \right. \\
& \left. + \left[\frac{d}{dt}(h_i \cos \theta_i) \right]^2 \right\} + \sum_{i=1}^N \frac{J_i \omega_i^2}{2} - \sum_{i=1}^N m_i g h_i (1 - \cos \theta_i), \quad (9)
\end{aligned}$$

where α is the rotation angle. After incorporating again the dissipation and driving, the equations of motion will become:

$$\ddot{\phi} = \frac{mr \cos(\alpha) \sum_i h_i \dot{\theta}_i^2 \sin \theta_i - c_{\phi} \dot{\phi} - \cos(\alpha) \sum_i M_i + A + B - C}{D}, \quad (10)$$

$$\ddot{\theta}_i = \frac{M_i - mr \cos(\alpha) \ddot{\phi} h_i \cos \theta_i - m g h_i \sin \theta_i - c_{\theta} \dot{\theta}_i}{m h_i^2 + J_i} \quad (11)$$

where

$$\begin{aligned}
A &= m^2 gr \cos(\alpha) \sum_i \frac{h_i^2 \sin \theta_i \cos \theta_i}{mh_i^2 + J_i}, \\
B &= mrc_\theta \cos(\alpha) \sum_i \frac{h_i \dot{\theta}_i \cos \theta_i}{mh_i^2 + J_i}, \\
C &= mr \cos(\alpha) \sum_i \frac{h_i M_i \cos \theta_i}{mh_i^2 + J_i}, \\
D &= \left[J + NmR^2 - m^2 r^2 \cos^2(\alpha) \sum_i \frac{h_i^2 \cos^2 \theta_i}{mh_i^2 + J_i} \right].
\end{aligned}$$

4.5.3 Numerical results

For solving Equations 10, 11 we used our previously written C program which uses velocity Verlet integration method with a $dt = 0.01$ s time-step. We carried out simulations for α values between 0^0 and 180^0 , varying α with a step of 1^0 . For each value of α we performed 100 program runs, computed the Kuramoto order parameter and averaged the results. The obtained graph in comparison to the experimental results can be seen in Fig 12.

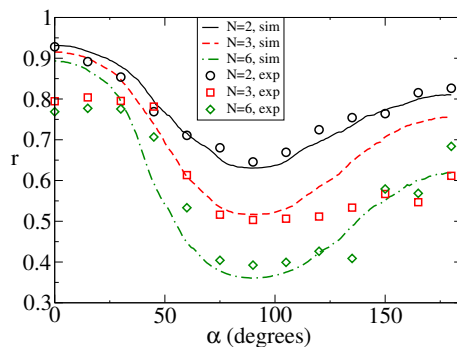


Figure 12: Comparison between the experimental and simulated results for the Kuramoto order parameter. The continuous lines correspond to the simulated results, and different symbols correspond to the experimental results.

When the number of metronomes are even ($N = 2$, $N = 6$), the experimental and theoretical results are in a good agreement. The differences for $N = 3$ case, is due to the fact that for $\alpha \in [90^0, 180^0]$ the experiments have shown that one metronome will shift continuously between two states. In one state it will be in phase with the other two and in the other it will be in anti-phase with the other two. This phenomenon is less frequently reproduced in the simulations, leading to a higher order parameter value.

After this validation of the model, our aim was to investigate the system for larger number of metronomes (up to $N = 100$). To illustrate the increased fluctuations in the neighborhood of the critical α value (the phase-transition point) we also calculated and plotted the standard deviation σ_r of the r order parameter for the 100 individual runs. The obtained results can be seen in Figure 13.

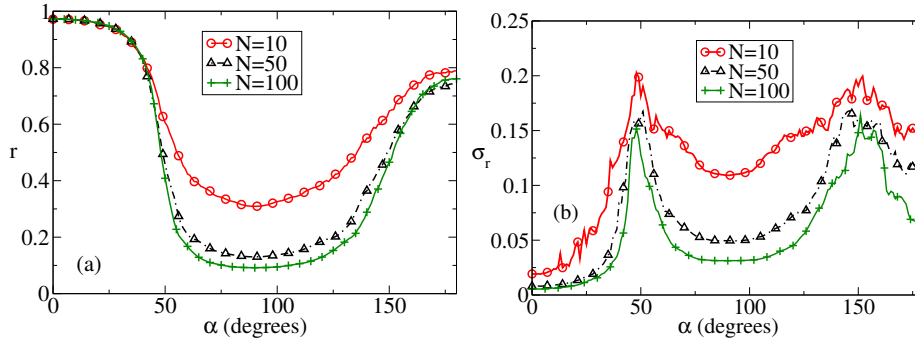


Figure 13: *Simulation results for larger metronome ensembles. (a) The synchronization order parameter as a function of the metronomes orientation. (b) The fluctuation of the order parameter as a function of the metronomes orientation on the disk.*

As we would expect, the transitions for larger systems are sharper and sharper, and the peak in the fluctuation of the order parameter also narrows for larger system size.

5 Summary

The dynamics of two different type of systems showing emergent synchronization was investigated by simple experiments and with computer simulations.

First a system composed from pulse emitting stochastic oscillators with two possible modes and a simple optimization dynamics was investigated. To prove the generality of synchronization models based on optimization, we considered two similar models: one with two possible waiting periods and one with two possible emitting periods. Here there is no explicitly built-in interaction which favors synchronization. Instead of this, there is a simple optimization rule governing the oscillators behavior, which tries to maintain the total output of the system, f around a certain f^* value. As a co-product of this simple optimization rule, synchronization emerges for certain f^* intervals. This nontrivial spontaneous synchronization appeared in both models studied by us, and the appearance and disappearance of spontaneous synchronization closely resembles a phase-transition. An experimental realization of this system was also considered. Even though our research is more a theoretical one, there could be several practical applications of it, like building oscillators with better period stability, or globally coupled CNN type computers.

As a second line of studies in the field of spontaneous synchronization, the collective behavior in a mechanical system composed from coupled metronomes placed on a freely rotating platform was investigated both by experiments

and computer simulations. In a first set of experiments we searched for the conditions which are favoring such synchronization. We came to the conclusion, that the obtained synchronization level will increase monotonically with the natural frequency of the metronomes. From the experimental data we found, that by increasing the number of metronomes in the system a decrease in the synchronization level will be obtained.

In order to investigate the system more thoroughly, a realistic model was built. We fixed the realistic model parameters and numerically integrated the equations of motion. The results offered by the model described well the experimental setup, and reproduced the experimentally observed results and trends. Through this model we managed to show the importance of the damping and driving in the appearance of the synchronization. From the simulations we came to the conclusion, that for an ensemble of metronomes with a fixed standard deviation of their natural frequencies, the order parameter increases as a function of the metronomes' average frequency, ω_0 . This increase happens sharply for large ensembles, closely resembling a phase-transition like phenomenon.

As a second set of experiments with this setup we investigated the influence of the coupling on the synchronization level. By rotating the metronomes swinging plane on the perimeter of the disk, the coupling strength can be finely tuned. As a function of the coupling strength, the system will exhibit an order-disorder type phase-transition, similar with the one known in the Kuramoto model. Our theoretical model with a few adjustments could be used to describe the new setup. The model reproduced well the experimental results and also allowed the study of much larger ensembles. For larger ensembles the transition in the order parameter becomes sharper in agreement with the expected trend for a phase-transition.

6 Relevant personal contributions

Personal contributions in the field of the two-mode stochastic oscillators:

1. I had written my own code for simulating the behavior of the oscillators for the original model and for the modified model;
2. I run the simulations and constructed the graphs;
3. I modified the programming of the electronic fireflies and performed all the experiments, as well had written codes to process the data. I also processed all the experimental data;
4. I helped in the construction of the experimental device.

Personal contributions in the study of the metronome system:

1. I helped in the construction of the experimental setup: together with one of my colleagues (B. Tyukodi) we mounted the light-gates and connected it with the circuit board;
2. I performed all the experiments, and had written the needed programs to interpret the results, processed the data and constructed the graphs;
3. Together with my supervisor we came up with two new models, and I had written the simulation programs to solve the involved equations.

Publications related to the Thesis

1. R. Sumi, Z. Nédá, A. Tunyagi, Sz. Boda and Cs. Szász. Nontrivial spontaneous synchronization. *Physical Review E*, 79:056205, 2009.
2. Zs. Sárközi, E. Káptalan, Z. Nédá, Sz. Boda and A. Tunyagi. Optimization induced collective behavior in a system of flashing oscillators. *International Journal of Bifurcation and Chaos*, 22:1230002, 2009.
3. Sz. Boda, Z. Nédá, B. Tyukodi and A. Tunyagi. The rhythm of coupled metronomes. *The European Physical Journal B*, 86:1, 2013.
4. Sz. Boda, Sz. Ujvári, A. Tunyagi and Z. Nédá, Kuramoto-type phase transition with metronomes, accepted in *European Journal of Physics* (2013)
5. Z. Nédá, Sz. Boda, and E. Káptalan, Rend a rendezetlenségéből - játék metronomokkal, accepted in *Természet világa* (2013)

Selected References

- [1] M. Bennet, M. F. Schatz, H. Rockwood, and K. Wiesenfeld. Huygens clocks. *Proceedings of the Royal Society A*, 458:563, 2002.
- [2] C. Huygens. Letter to de sluse, in: Oeuvres complètes de christian huygens. *Societe Hollandaise Des Sciences*, 1665.
- [3] Ch. Huygens. *Evres Completes*. Swets and Zeitlinger B.V., Amsterdam, 1967.
- [4] M. Kapitaniak, K. Czolczynski, P. Perlikowski, A. Stefanski, and T. Kapitaniak. Synchronization of clocks. *Physics Reports*, 517:1–69, 2012.
- [5] Y. Kuramoto and I. Nishikawa. Statistical macrodynamics of large dynamical systems. case of a phase transition in oscillator communities. *Journal of Statistical Physics*, 49:569, 1987.
- [6] Martha K. McClintock. Menstrual synchrony and suppression. *Nature*, 229:244, 1971.
- [7] R. Mirollo and S. Strogatz. Synchronization of pulse-coupled biological oscillators. *SIAM Journal on Applied Mathematics*, 50:775, 1990.
- [8] Z. Néda, A. Nikitin, and T. Vicsek. Synchronization of two-mode stochastic oscillators: a new model for rhythmic applause and much more. *Physica A*, 321:238, 2003.
- [9] Z. Néda, E. Ravasz, Y. Brechet, T. Vicsek, and A.-L. Barabási. Self-organizing processes: The sound of many hands clapping. *Nature*, 403:849, 2000.
- [10] J. Pantaleone. Synchronization of metronomes. *American Journal of Physics*, 70:992, 2002.
- [11] C. S. Peskin. *Mathematical Aspects of Heart Physiology*. Courant Institute of Mathematics, New York, 1975.
- [12] H. M. Smith. Synchronous flashing of fireflies. *Science*, 16:151, 1935.

- [13] S. Strogatz. From kuramoto to crawford: exploring the onset of synchronization in populations of coupled oscillators. *Physica D*, 226:181–196, 2000.
- [14] S. Strogatz. *Sync: The Emerging Science of Spontaneous Order*. Hyperion, New York, 2003.
- [15] H. Ulrichs, A. Mann, and U. Parlitz. Synchronization and chaotic dynamics of coupled mechanical metronomes. *Chaos*, 19:043120, 2009.
- [16] A. T. Winfree. Biological rhythms and the behavior of coupled oscillators. *Journal of Theoretical Biology*, 16:15, 1967.